EAST EUROPEAN JOURNAL OF PHYSICS. 3. 390-397 (2025)
DOI:10.26565/2312-4334-2025-3-40 ISSN 2312-4334

IMPACT OF BORON DOPING ON CHARGE DISTRIBUTION AND THERMAL CONDUCTIVITY IN DOUBLE-WALLED CARBON NANOTUBES

Shahnozakhon Muminova[a], Abror Ulukmuradov[b], Xamid Isayev[b], Dildora Mamayeva[b], Utkir Uljayev[a,b]*

[a]*Denov Institute of Entrepreneurship and Pedagogy, 360 Denov City, Surkhandarya Region, 190507, Uzbekistan*
[b]*Tashkent Institute of Textile and Light Industry, Tashkent, 100100, Uzbekistan*
**Corresponding Author E-mail: utkir.uljaev@outlook.com*
Received April 24, 2025; revised August 7, 2025; accepted August 15, 2025

This study investigates the effect of boron (B) doping on the electrical and thermal conductivity properties of single-walled carbon nanotubes (DWNTs) at various temperatures (300 K to 1500 K). The incorporation of boron atoms into DWNTs (5,5)@(10,10) was analyzed to explore how different doping levels (ρ%) influence the partial charge distribution and thermal conductivity. Our findings show that boron doping increases the partial charge within the nanotube structure, with a nonlinear increase in charge as the doping concentration rises from 0% to 10%. This is due to the lower electronegativity of boron, which introduces hole carriers and enhances *p*-type semiconductor behavior. However, at higher doping concentrations (above 5%), defects disrupt the π-electron network, reducing electrical conductivity. Thermal conductivity experiments indicate that the presence of boron leads to a decrease in heat transfer efficiency, especially at higher doping levels (>6%), where defect-induced phonon scattering significantly reduces the thermal conductivity. The results demonstrate that boron doping has a complex impact on the structural, electronic, and thermal properties of DWNTs, with temperature and doping concentration playing critical roles in determining performance.
Keywords: *Double-walled carbon nanotube; Boron doping; Reactive molecular dynamics*
PACS: 61.46.-w, 02.70.Ns

1. INTRODUCTION

Carbon nanotubes (CNTs), a type of carbon-based nanostructure, continue to garner substantial research interest, with the body of literature on the topic growing at an exponential rate [1,2]. The carbon nanotubes (CNT) are tubular-shaped one-dimensional sp^2-hybridized carbon atoms arranged on honeycomb lattices. Since the rediscovery of CNTs by Iijima [3], it is one of the most explored nanomaterials. CNTs are classified as single-, double-, or multi-walled structures, exhibiting either semiconductor (S) or metallic (M) behavior based on their chiral indices. Approximately 60% of all nanotube chiralities are semiconductors, while the remaining 40% are metals [4]. Various types of nanotubes include Carbon Nanotubes (CNTs) [5], Boron Nitride Nanotubes (BNNTs) [6], Silicon Nanotubes (SiNTs) [7], and Hybrid Nanotubes (such as B-CNT and N-CNT, which integrate materials like carbon and boron nitride for multifunctional properties) [8]. These nanotubes, celebrated for their unique properties, have a wide range of applications in microelectronics [8], energy storage [9], sensors [10], and drug delivery [11]. They garner interest across various fields, including physics, chemistry, and materials science [12], showcasing their potential in electronic devices [13], sensors [14], adsorbents [9,15], and numerous other applications.

Various approaches, including functionalization, enable the customization of CNT properties [16]. Functionalization, accomplished through substitution reactions with comparable heteroatoms or functional groups, modifies CNTs' solubility, chemical reactivity, and various other physicochemical characteristics [17]. Notably, functionalization aids in the isolation of nanotube bundles. Consequently, studies have extensively explored CNT interactions with atoms and molecules like boron (B) [18], nitrogen (N) [19], calcium (Ca) [20], palladium (Pd) [21], fluorine (F) [22], bromine [23], and platinum (Pt) [24].

In recent years, boron-doped carbon nanotubes (B-CNTs) have garnered increasing interest due to their exceptional properties and wide-ranging applications [25]. Boron doping introduces alterations to the electronic structure of carbon nanotubes, enhancing their conductivity, catalytic activity, and chemical reactivity [26]. These unique characteristics make B-CNTs highly suitable for applications in energy storage [9], sensing, catalysis and nanotechnology [27]. B-doping of pristine CNTs offers the possibility to transform semiconducting tubes into metallic tubes by lowering the Fermi level into a valance band [28]. It also alters the crystallinity and stiffness of CNTs [29]. Furthermore, the incorporation of boron atoms modifies the band gap of carbon nanotubes, offering tailored properties for specific functional requirements. Therefore, boron (B) remain the preferred elements for substitution reactions [30].

Boron serves as a *p*-type dopant, enhancing nanotube growth by increasing oxidation resistance [31]. The similar atomic sizes of boron and carbon enable their seamless incorporation into the graphite network. Methods used to produce B-CNTs include carbon arc, laser ablation [32], substitution reactions [33], and chemical vapor deposition (CVD) [34]. For instance, Han et al. [35] successfully synthesized B-CNTs via substitution reactions (with a B/C ratio

Cite as: Sh. Muminova, A. Ulukmuradov, X. Isayev, D. Mamayeva, U. Uljayev, East Eur. J. Phys. 3, 390 (2025), https://doi.org/10.26565/2312-4334-2025-3-40

of 4.17), while Chen et al. [36] utilized microwave plasma CVD with trimethyl borate as a doping source. Additionally, Wang et al. [37] fabricated B-CNTs using electron cyclotron resonance chemical vapor deposition (ECR-CVD) on porous silicon substrates. Despite these advancements, precise control over the boron content in CNT structures remains challenging. Boron not only supports nanotube growth [38] but also enhances oxidation resistance [39], making it valuable for adjusting nanotube morphology and properties. The comparable atomic sizes of boron and carbon facilitate their integration into the graphite network. Therefore, B appears to have additional properties in terms of controlling the morphology and properties of nanotubes. CNTs are grown from boron or its compounds using various techniques (e.g., CVD, ALD) [40] and their various properties (i.e., mechanical, optical, electrical) are being studied.

In this study, we investigated molecular dynamics (MD) methods to calculate the electronic and thermal properties of boron-doped double carbon nanotubes (B-DWNT).

2. COMPUTATIONAL DETAILS

We investigate the process of boron (B) doped onto DWNTs (B-DWNTs) through reactive MD simulations employing the LAMMPS package [41]. The ReaxFF potential describes interatomic interactions, accounting for bond breaking and formation [42]. The most commonly used chiral DWNTs in other research studies (5,5)@(10,10) were selected as model system [43,44]. Our model includes pristine metal (5,5)@(10,10) nanotubes, denoted as B-DWNT(5,5)@(10,10) in MD simulations (Fig.1). Selected nanotubes diameters 13.64 Å-13.57 Å for (5,5)@(10,10) fall within experimentally observed ranges (13-16 Å) [45,46]. We apply periodic boundary conditions along the z-axis, allowing simulation of infinitely long B-DWNTs with lengths of 28.12 Å for B-DWNT(5,5)@(10,10) respectively. The (5,5)@(10,10) chiral DWNTs consist of 600 C atoms, respectively, with a B content of 0 to 10% (Fig.1).

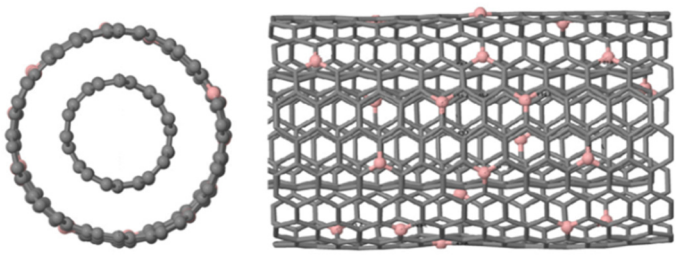

Figure 1. Top and side views of the B-DWNT(5,5)@(10,10) model system. Carbon (C) and Boron (B) atoms are shown in gray and coral, respectively

Initially, we minimize the energy of all model systems using the conjugate gradient method. Subsequently, we equilibrate system temperature and pressure to desired values (300 K, 600 K, 900 K, 1200, 1500 K and 0 Pa) in the NpT ensemble employing a Berendsen thermostat and barostat [47]. Our chosen heating rate (1 K/ps) aligns with previously reported values (0.1–10.0 K/ps) [48] ensuring insignificant deviations in thermodynamic equilibrium during temperature changes. For chemisorption of B atoms on DWNTs, we maintain system temperature at 300-1500 K for 100 ps using a Bussi thermostat [49]. Modeling was performed in the NVE ensemble to determine the heat transfer coefficient in the systems. Since the DWNTs were considered to be infinite in the modeling based on the periodicity conditions, the heat transfer was evaluated not by the number of B atoms, but by the content (%) of B atoms.

Initially, the electrical conductivity (partial charge) of the doped B atoms is calculated according to their amount (ρ,%) and temperature (300-1500 K). We estimate the amount (%) of doped B atoms on the surfaces of pure DWNTs at different temperatures (300 K, 600 K, 900 K, 1200 and 1500 K) as follows:

$$\rho = \frac{\text{number of atoms doped } (N_B)}{\text{total atoms in a pristine DWNT } (N_C)} * 100\%, \quad (1)$$

where, N_B- number of doping boron (B) and N_C- number of carbon atoms.

In addition, the thermal conductivity coefficient was determined using the Green-Kubo formula [50]:

$$k = \frac{1}{3Vk_BT^2}\int_0^\infty \langle J(0)\cdot J(t)\rangle dt, \quad (1)$$

where V is the system volume, k_B Boltzmann constant, T temperature, The angle brackets $\langle --\rangle$ represent the average value of the heat flux autocorrelation function $J(t)$ over all atoms. The heat flux $J(t)$ is determined by the following formula:

$$J(t) = \frac{1}{2V}\sum_{i=1}^{N}\sum_{j=1}^{N} r_{ij}\cdot(F_{ij}\cdot v_i), \quad (3)$$

where r_{ij} and F_{ij} represent the distance and force between atoms i and j, and v_i represents the velocity of atom i.

In all cases MD time step is 0.1 fs. The simulations are conducted 10 times for each study case, and the results are obtained by averaging the corresponding physical quantities

RESULTS AND DISCUSSION

Electrical conductivity (partial charge)

When carbon nanotubes (CNTs) are grown with boron (B) at different temperatures, several factors come into play that can affect their structure, properties, and performance. From current literature, boron incorporation into carbon materials requires a high carbonization temperature of about 600-1100 °C (873-1373 K) [51]. The effect of boron on CNTs at low temperatures results in a high density of defects, leading to decreased electrical and thermal properties. Conversely, the addition of boron at high temperatures enhances thermal stability and improves electrical and mechanical properties [52].

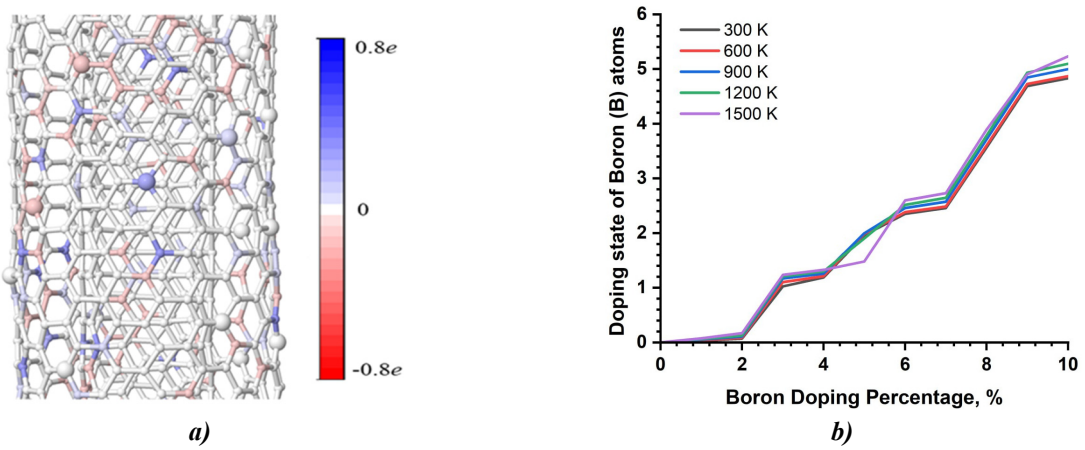

a) *b)*

Figure 2. (*a*) B atoms doping onto DWNT(5,5)@(10,10) are introduced, and system atoms exhibit partial charges from -0.8*e* to +0.8*e*, which range from red to blue is depicted by the color spectrum, which shows the transition from electron-rich regions to electron-poor regions, respectively, (*b*) The alteration in the partial charge of adsorbed B atoms in relation to temperature

Therefore, this study investigated the effect of B-DWNTs at selected temperatures of 300 K, 600K, and 900 K, 1200 K, 1500 K. The results indicate variations in the doping of B atoms on the surfaces of DWNT(5,5)@(10,10) at different temperatures (i.e., 300 K, 600 K, 900 K, 1200 K, 1500 K). Various factors influence the chemisorption of B atoms on DWNTs, including the nanotube surface curvature and the arrangement of carbon rings [53,54]. The doped coverage varies with temperature, and depending on their position within the hexagonal cell of the CNT, B atoms may detach from the surface due to temperature effects [55,56]. B atoms doping on the surface of DWNTs are affected by the arrival of other B atoms on the surface. This can result in the formation of molecules through the Langmuir-Hinshelwood recombination mechanism, where two B atoms on the surface covalently bond to form a B molecule. The temperature range (300-1500 K) employed in this study alters the quantity of B atoms doped on the surface [57,58].

Atoms in the system are color-coded to represent positive charges in blue and negative charges in red, while uncharged atoms are depicted in white (Fig. 2*a*). In this study, the charge distribution in the system changes with temperatures corresponding to ρ % of B atoms added in DWNT. In particular, the change in the partial charge in the system with an increase in ρ % in the temperature range from 300 K to 1500 K is shown in Figure 2*b*. It can be seen from the results that the partial charge in the system also increases nonlinearly with an increase in ρ %. One of the reasons for the non-linear increase may be related to the gravitational force used to calculate the interactions between the partial atoms [43]. The difference in electronegativity results in a variation in partial charges of carbon nanotube (CNT) and B atoms. Specifically, with increasing ρ % (i.e., from 300 K to 1500 K), the partial charging in DWNT increases due to the lower electronegativity of B (2.04) compared to carbon (2.55), causing it to lose electrons and generate a positive partial charge. That is, as the doping concentration (ρ %) increases, the number of boron atoms increases, leading to more changes in the electron distribution within the DWNT structure. This enhances the interaction with neighboring carbon atoms and other boron atoms, resulting in an increase in partial charge. The partial charge of B atoms in B-DWNT(5,5@10,10) increased from approximately 1%) to approximately 5.833e (10%) in the doped state (at temperatures between 300 and 1500 K) for 300 K, while in the case B-DWNT(5,5@10,10) nanotubes, the values increased from ~0.041*e* (1%) to ~5.868*e* (10%), respectively, at a temperature of 600K. At 900K, the values increased from ~0.065*e* (1%) to ~6.096*e* (10%). At 1200K, the increase was from ~0.065*e* (1%) to ~5.096*e* (10%). Finally, at 1500K, the change was from ~0.0674*e* (1%) to ~5.233*e* (10%) (Table 1).

Table 1. Partial charge variation with boron (B) atom doping at different temperatures for B-DWNT(5,5@10,10)

Boron doping (%)	**Partial charge, *e***				
	(5,5@10,10)				
	300 K	**600 K**	**900 K**	**1200 K**	**1500 K**
1	0.032	0.041	0.053	0.065	0.074
7	2.457	2.484	2.572	2.646	2.728
10	4.830	4.867	4.996	5.096	5.233

This indicates that an increase in the concentration of B leads to an increase in positive partial charges of the DWNT. This validates the outcomes achieved in earlier investigations [40]. B-DWNTs (DWNT(5,5)@(10,10) doped with B atoms and subjected to different temperatures, then the changes in their partial charges (*e*) are compared (*Supplementary information*).

The results indicate that at low boron doping (<1%), the increase in partial charge is not very significant (Fig. 2*b*). This is because low boron atoms create defects in the carbon lattice, which limits the free movement of π-electrons. As a result, electrical conductivity decreases due to increased scattering of charge carriers. As the doping of B atoms increases (1-5%), a slight increase in the partial charge in the B-DWNT system was observed (at 300-900 K). Since boron has a lower electronegativity than carbon, it introduces hole carriers into the structure, enhancing the *p*-type semiconductor properties of the B-DWNT. Under these conditions, electrical conductivity can increase. At high boron doping (>5%), a sharp decrease in the partial charge was observed. At very high boron concentrations (>8%), the π-electron network of the carbon nanotube is disrupted, and the excess defects lead to scattering of charge carriers. In this study, the average lengths of C-C and B-C bonds were found to be 1.426 and 1.514 Å, respectively, thus supporting the conclusion mentioned earlier [26].

Generally, the low electronegativity of boron introduces hole carriers, resulting in positive partial charges and *p*-type behavior in DWNTs.

Variation in thermal conductivity (*k*)

Figure 3 shows the thermal conductivity coefficient for (5,5@10,10) doped with different amounts (*ρ*%) of boron (B) as a function of temperature (300-1500 K).

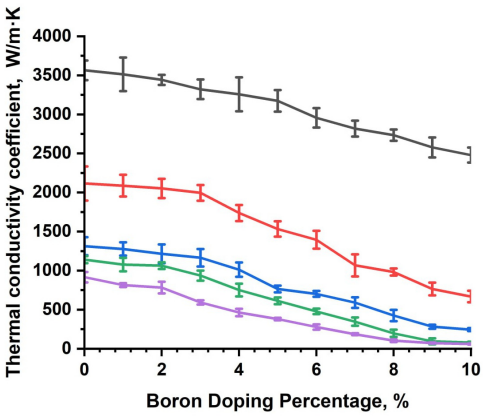

Figure 3. The variation of the thermal conductivity coefficient with doping amount and temperature

When analyzing the thermal conductivity (*k*) as a function of B doping concentration in B-DWNTs, at 300 K, *k* decreased noticeably by a factor of 1.012 at 1% (1%) B doping compared to the undoped case. At 600 K, the reduction was even greater, with k decreasing by a factor of 1.013. At higher temperatures 900 K, 1200 K, and 1500 K the thermal conductivity dropped by factors of 1.028, 1.058, and 1.124, respectively (Table 2). As the doping concentration *ρ*% of B atoms increases, thermal conductivity *k* also varies with temperature (*see Supplementary Information*).

Table 2. Thermal conductivity variation with boron (B) atom doping at different temperatures for B-DWNT(5,5@10,10)

Boron doping (%)	**Thermal conductivity coefficient (W/m·K)**				
	5,5@10,10				
	300 K	**600 K**	**900 K**	**1200 K**	**1500 K**
0	3564	2115	1313	1140	916
1	3512	2087	1277	1077	815
3	3321	1995	1165	936	593
5	3173	1533	764	613	379
8	2734	982	425	197	103
10	2479	668	245	78	61

Specifically, for B-DWNT(5.5@10.10), at temperatures of 300 K and 900 K, the thermal conductivity *k* at 1% doping is 3512 W/m•K and 1277 W/m•K, respectively. Likewise, at 1200 K and 1500 K, the difference increases, with k being 1.14 times and 1.30 times greater, respectively.

Overall, as the concentration of doped B atoms increases, the thermal conductivity of the two nanotubes begins to diverge. This behavior is primarily due to the weak phonon-electron interaction of boron. At 300 K, an initial increase in boron concentration (*ρ*%) in the DWNT structure results in a slight rise in thermal conductivity (by more than 3%), followed by a gradual decline (exceeding 4%). When B doping reaches 4–5%, the thermal conductivity drops significantly.

One contributing factor is the increased presence of structural defects, which sharply enhances phonon scattering-phonons being the primary heat carriers in carbon nanotubes. As the B doping concentration (ρ%) rises, so does the number of defects, leading to greater phonon scattering and reduced heat transfer.

When B doping falls within the 6%-10% range, structural disorder becomes more pronounced, resulting in a significant drop in thermal conductivity. At 10% boron doping, particularly in B-DWNT(5.5@10.10), thermal conductivity nearly reaches its minimum due to maximum phonon scattering and a sharp decline in transport efficiency. Notably, across nearly all temperature ranges (300-1500 K), the decline in thermal conductivity typically begins around 7%–8% doping.

Overall, at moderate temperatures (300–400 K), increased phonon interactions amplify the influence of boron doping on thermal conductivity, resulting in a slight decrease in thermal conductivity as boron content rises. For instance, B-DWNTs doped with 1% boron exhibit higher thermal conductivity compared to those with 2% or 3% doping. At elevated temperatures (T > 500 K), phonon-phonon scattering becomes the dominant mechanism, leading to a reduction in thermal conductivity regardless of the doping level. However, in heavily doped B-DWNTs (>6%), thermal conductivity is significantly lower due to the inability of lattice vibrations to propagate effectively amid excessive structural defects. As a result, the system's thermal conductivity varies with changes in external temperature. Boron doping creates defects and disrupts the phonon transport network in DWNTs, leading to increased phonon scattering and a reduction in thermal conductivity, particularly at high doping concentrations.

CONCLUSION

The results demonstrate that the intentional introduction of boron atoms into DWNTs leads to changes in both electrical and thermal conductivity, specifically an increase in electrical conductivity (partial charge) and a decrease in thermal conductivity (k). The average partial charge (e) in the B-DWNT system increased from 0.032e to 4.830e at 300 K for B-DWNT(5.5@10.10) as the B content (ρ%) rose. Between 600 K and 1500 K, the increase in ρ% was 2.31 and 2.56 times greater (at 1% and the 1500 K/300 K ratio), respectively, while the increase in partial charge was 1.11 and 1.15 times greater (at 7% and the 1500 K/300 K ratio). At the maximum B doping level (10%), the partial charge increased by 1.08 and 1.09 times, respectively. Therefore, the increase in partial charge with rising ρ% in B-DWNTs can be attributed to a combination of electronic distribution, thermal effects, structural changes, and ionic effects.

At room temperature (300 K), the thermal conductivity of 1% doped B-DWNTs is approximately 3564 W/mK for (5.5@10.10) and 3651 W/mK. As the boron content (ρ%) increases, the thermal conductivity of (5.5@10.10) chiral B-DWNTs decreases more than that of. Specifically, when 7% boron is added to (5.5@10.10) chiral B-DWNTs and 6.75% boron is, their thermal conductivity decreases by 1.26 times, respectively, compared to the 0% case. These results demonstrate the potential for modifying the electrical and thermal conductivity of DWNTs through boron doping, enhancing their suitability for use in thermal interface materials (TIMs).

Acknowledgment

This research was carried out within the framework by the fundamental research program of the Academy Sciences of Uzbekistan.

ORCID

Abror Ulukmuradov, https://orcid.org/0000-0002-7135-9673; **Utkir Uljayev,** https://orcid.org/0009-0002-2564-5270

REFERENCES

[1] S. Iijima, "Carbon nanotubes: past, present, and future," Phys. B: Condens. Matter **323**, 1-5 (2002). https://doi.org/10.1016/S0921-4526(02)00869-4

[2] S. Rathinavel, K. Priyadharshini, and D. Panda, "A review on carbon nanotube: An overview of synthesis, properties, functionalization, characterization, and the application," Mater. Sci. Eng. B **268**, 115095 (2021). https://doi.org/10.1016/j.mseb.2021.115095

[3] S. Iijima, "Helical microtubules of graphitic carbon," Nature **354**, 56-58 (1991). https://doi.org/10.1038/354056a0

[4] K.E. Moore, D.D. Tune, and B.S. Flavel, "Double-Walled Carbon Nanotube Processing," Adv. Mater. **27**, 3105 (2015). https://doi.org/10.1002/adma.201405686

[5] N. Anzar, R. Hasan, M. Tyagi, N. Yadav, and J. Narang, "Carbon nanotube - A review on Synthesis, Properties and plethora of applications in the field of biomedical science," Sens. Int. **1**, 100003 (2020). https://doi.org/10.1016/j.sintl.2020.100003

[6] J.H. Kim, T.V. Pham, J.H. Hwang, C.S. Kim, and M.J. Kim, "Boron nitride nanotubes: synthesis and applications, Nano Converg. **5**, 17 (2018). https://doi.org/10.1186/s40580-018-0149-y

[7] P. Castrucci, M. Scarselli, M. De Crescenzi, M. Diociaiuti, Prajakta S. Chaudhari, C. Balasubramanian, *et al*., "Silicon nanotubes: Synthesis and characterization," Thin Solid Films, **508**(1-2), 226-230 (2006), https://doi.org/10.1016/j.tsf.2005.07.348

[8] S.V. Sawant, A.W. Patwardhan, J.B. Joshi, and K. Dasgupta, "Boron doped carbon nanotubes: Synthesis, characterization and emerging applications – A review," Chem. Eng. J. **427**, 131616 (2022). https://doi.org/10.1016/j.cej.2021.131616

[9] U. Khalilov, U. Uljayev, K. Mehmonov, P. Nematollahi, M. Yusupov, and E. Neyts, "Can endohedral transition metals enhance hydrogen storage in carbon nanotubes?" Int. J. Hydrog. Energy, **55**, 604-610 (2024). https://doi.org/10.1016/j.ijhydene.2023.11.195

[10] U.B. Uljaev, S.A. Muminova, and I.D. Yadgarov, "Nitrogen Adsorption on Double-Walled Carbon Nanotube at Different Temperatures: Mechanistic Insights from Molecular Dynamics Simulations," East Eur. J. Phys. (1), 361-365 (2024). https://doi.org/10.26565/2312-4334-2024-1-34

[11] M.F. Naief, S.N. Mohammed, H.J. Mayouf, and A.M. Mohammed, "A review of the role of carbon nanotubes for cancer treatment based on photothermal and photodynamic therapy techniques," J. Organomet. Chem. **999**, 122819 (2023). https://doi.org/10.1016/j.jorganchem.2023.122819
[12] A. Ali, S.S. Rahimian Koloor, A.H. Alshehri, and A. Arockiarajan, "Carbon nanotube characteristics and enhancement effects on the mechanical features of polymer-based materials and structures – A review," J. Mater. Res. Technol. **24**, 6495-6521 (2023). https://doi.org/10.1016/j.jmrt.2023.04.072
[13] M. Soto, T.A. Boyer, S. Biradar, L. Ge, R. Vajtai, A. Elías-Zúñiga, P.M. Ajayan, and E.V. Barrera, "Effect of interwall interaction on the electronic structure of double-walled carbon nanotubes," Nanotechnology, **26**, 165201 (2015). https://doi.org/10.1088/0957-4484/26/16/165201
[14] Y. Yao, R. Shen, J. Xu, and Z. Feng, "Progress in electrochemical sensing of epinephrine using carbon nanomaterials: A review," Int. J. Electrochem. Sci. **19**, 100750 (2024). https://doi.org/10.1016/j.ijoes.2024.100750
[15] M. Sajid, M. Asif, N. Baig, M. Kabeer, I. Ihsanullah, and A.W. Mohammad, "Carbon nanotubes-based adsorbents: Properties, functionalization, interaction mechanisms, and applications in water purification," J. Water Process Eng. **47**, 102815 (2022). https://doi.org/10.1016/j.jwpe.2022.102815
[16] D. Liu, L. Shi, Q. Dai, X. Lin, R. Mehmood, Z. Gu, and L. Dai, "Functionalization of carbon nanotubes for multifunctional applications," Trends Chem. **6**, 186-210 (2024). https://doi.org/10.1016/j.trechm.2024.02.002
[17] M. Adamska, and U. Narkiewicz, "Fluorination of Carbon Nanotubes − A Review," J. Fluor. Chem. **200**, 179-189 (2017). https://doi.org/10.1016/j.jfluchem.2017.06.018
[18] D. Silambarasan, V.J. Surya, V. Vasu, and K. Iyakutti, "Experimental investigation of hydrogen storage in single walled carbon nanotubes functionalized with borane," Int. J. Hydrog. Energy, **36**, 3574-3579 (2011). https://doi.org/10.1016/j.ijhydene.2010.12.028
[19] Y. Tison, *et al*., "Identification of Nitrogen Dopants in Single-Walled Carbon Nanotubes by Scanning Tunneling Microscopy," ACS Nano, **7**, 7219-7226 (2013). https://doi.org/10.1021/nn4026146
[20] S.H. De Paoli Lacerda, J. Semberova, K. Holada, O. Simakova, S. D. Hudson, and J. Simak, "Carbon Nanotubes Activate Store-Operated Calcium Entry in Human Blood Platelets," ACS Nano, **5**, 5808-5813 (2011). https://doi.org/10.1021/nn2015369
[21] H. Wu, D. Wexler, and H. Liu, "Effects of different palladium content loading on the hydrogen storage capacity of double-walled carbon nanotubes," Int. J. Hydrog. Energy **37**, 5690 (2012). https://doi.org/10.1016/j.ijhydene.2011.12.120
[22] L.G. Bulusheva, Y.V. Fedoseeva, E. Flahaut, J. Rio, C.P. Ewels, V.O. Koroteev, G. Van Lier, *et al*., "Effect of the fluorination technique on the surface-fluorination patterning of double-walled carbon nanotubes," Beilstein J. Nanotechnol. **8**, 1688-1698 (2017). https://doi.org/10.3762/bjnano.8.169
[23] L.G. Bulusheva, A.V. Okotrub, E. Flahaut, I.P. Asanov, P.N. Gevko, V.O. Koroteev, Yu.V. Fedoseeva, *et al*., "Bromination of Double-Walled Carbon Nanotubes," Chem. Mater. **24**, 2708-2715 (2012). https://doi.org/10.1021/cm3006309
[24] D. Xia, Y. Luo, Q. Li, Q. Xue, X. Zhang, C. Liang, and M. Dong, "Extracting the inner wall from nested double-walled carbon nanotube by platinum nanowire: molecular dynamics simulations," RSC Adv. **7**, 39480 (2017). https://doi.org/10.1039/C7RA07066G
[25] U. Uljayev, S. Muminova, K. Mehmonov, I. Yadgarov, and A. Ulukmuradov, "Boron interaction with double-walled carbon nanotubes across temperature ranges," Mod. Electron. Mater. **10**, 3 (2024). https://doi.org/10.3897/j.moem.10.3.131526
[26] S.V. Boroznin, "Carbon nanostructures containing boron impurity atoms: synthesis, physicochemical properties and potential applications," Mod. Electron. Mater. **8**, 23-42 (2022). https://doi.org/10.3897/j.moem.8.1.84317
[27] M. Sireesha, V.J. Babu, A.S. Kiran, and S. Ramakrishna, "A review on carbon nanotubes in biosensor devices and their applications in medicine," Nanocomposites **4**, 36 (2018). https://doi.org/10.1080/20550324.2018.1478765
[28] L. Wirtz, and A. Rubio, "Band structure of boron doped carbon nanotubes," **685**, 402-405 (2003). https://doi.org/10.1063/1.1628059
[29] J. Saloni, W. Kolodziejczyk, S. Roszak, D. Majumdar, G. Hill, Jr., J. Leszczynski, "Local and Global Electronic Effects in Single and Double Boron-Doped Carbon Nanotubes," J. Phys. Chem. C, **114**(3), 1528–1533 (2010). https://doi.org/10.1021/jp910625w
[30] D. Jana, C.-L. Sun, L.-C. Chen, and K.-H. Chen, "Effect of chemical doping of boron and nitrogen on the electronic, optical, and electrochemical properties of carbon nanotubes," Prog. Mater. Sci. **58**, 565-635 (2013). https://doi.org/10.1016/j.pmatsci.2013.01.003
[31] T.-J. Li, *et al*., "Boron-doped carbon nanotubes with uniform boron doping and tunable dopant functionalities as an efficient electrocatalyst for dopamine oxidation reaction," Sens. Actuators B: Chem. **248**, 288-297 (2017). https://doi.org/10.1016/j.snb.2017.03.118
[32] P. Ayala, J. Reppert, M. Grobosch, M. Knupfer, T. Pichler, and A. Rao, "Evidence for substitutional boron in doped single-walled carbon nanotubes," Appl. Phys. Lett. **96**, 183110 (2010). https://doi.org/10.1063/1.3427432
[33] S. Parham, *Heteroatom-Doped Carbon Allotropes in Solar Cells Application*, in *Heteroatom-Doped Carbon Allotropes: Progress in Synthesis, Characterization, and Applications*, vol. 1491, (American Chemical Society, 2024), pp. 127–149.
[34] S.V. Sawant, S. Banerjee, A.W. Patwardhan, J.B. Joshi, and K. Dasgupta, "Effect of in-situ boron doping on hydrogen adsorption properties of carbon nanotubes," Int. J. Hydrog. Energy **44**, 18193-18204 (2019). https://doi.org/10.1016/j.ijhydene.2019.05.029
[35] W. Han, Y. Bando, K. Kurashima, and T. Sato, "Synthesis of boron nitride nanotubes from carbon nanotubes by a substitution reaction," Appl. Phys. Lett. **73**, 3085-3087 (1998). https://doi.org/10.1063/1.122680
[36] C.F. Chen, C.L. Tsai, and C.L. Lin, "The characterization of boron-doped carbon nanotube arrays," Diam. Relat. Mater. **12**, 1500-1504 (2003). https://doi.org/10.1016/S0925-9635(03)00181-X
[37] Z. Wang, C.H. Yu, D. Ba, and J. Liang, "Influence of the gas composition on the synthesis of boron-doped carbon nanotubes by ECR-CVD," Vacuum, **81**, 579-582 (2007). https://doi.org/10.1016/j.vacuum.2006.05.012
[38] X. Blase, J.-C. Charlier, A. De Vita, R. Car, Ph. Redlich, M. Terrones, W. K. Hsu, *et al*., "Boron-Mediated Growth of Long Helicity-Selected Carbon Nanotubes," Phys. Rev. Lett. **83**, 5078 (1999). https://doi.org/10.1103/PhysRevLett.83.5078

[39] L.E. Jones, and P.A. Thrower, "Influence of boron on carbon fiber microstructure, physical properties, and oxidation behavior," Carbon, **29**, 251-269 (1991). https://doi.org/10.1016/0008-6223(91)90076-U
[40] M. Terrones, A. Jorio, M. Endo, A.M. Rao, Y.A. Kim, T. Hayashi, H. Terrones, *et al*., New direction in nanotube science, Mater. Today **7**, 30 (2004). https://doi.org/10.1016/S1369-7021(04)00447-X
[41] A.P. Thompson, *et al*., "LAMMPS - a flexible simulation tool for particle-based materials modeling at the atomic, meso, and continuum scales," Comput. Phys. Commun. **271**, 108171 (2022). https://doi.org/10.1016/j.cpc.2021.108171
[42] J.E. Mueller, A.C.T. van Duin, and W.A.I. Goddard, "Development and Validation of ReaxFF Reactive Force Field for Hydrocarbon Chemistry Catalyzed by Nickel," J. Phys. Chem. C **114**, 4939-4949 (2010). https://doi.org/10.1021/jp9035056
[43] J.R. Lukes, and H. Zhong, "Thermal Conductivity of Individual Single-Wall Carbon Nanotubes," J. Heat Transf. **129**, 705-716 (2007). https://doi.org/10.1115/1.2717242
[44] A.T. Zahra, A. Shahzad, A. Manzoor, J. Razzokov, Q.U.A. Asif, K. Luo, and G. Ren, "Structural and thermal analyses in semiconducting and metallic zigzag single-walled carbon nanotubes using molecular dynamics simulations," PLOS ONE **19**, e0296916 (2024). https://doi.org/10.1371/journal.pone.0296916
[45] G. Chen, S. Bandow, E.R. Margine, C. Nisoli, A.N. Kolmogorov, V.H. Crespi, R. Gupta, G.U. Sumanasekera, *et al.*, "Chemically Doped Double-Walled Carbon Nanotubes: Cylindrical Molecular Capacitors," Phys. Rev. Lett. **90**, 257403 (2003). https://doi.org/10.1103/PhysRevLett.90.257403
[46] K. Mehmonov, A. Ergasheva, M. Yusupov, and U. Khalilov, "The role of carbon monoxide in the catalytic synthesis of endohedral carbyne," J. Appl. Phys. **134**, 144303 (2023). https://doi.org/10.1063/5.0160892
[47] H.J.C. Berendsen, J.P.M. Postma, W.F. Van Gunsteren, A. DiNola, and J.R. Haak, "Molecular dynamics with coupling to an external bath," J. Chem. Phys. **81**, 3684-3690 (1984). https://doi.org/10.1063/1.448118
[48] J. Sun, P. Liu, M. Wang, and J. Liu, "Molecular Dynamics Simulations of Melting Iron Nanoparticles with/without Defects Using a Reaxff Reactive Force Field," Sci. Rep. **10**, 3408 (2020). https://doi.org/10.1038/s41598-020-60416-5
[49] G. Bussi, D. Donadio, and M. Parrinello, "Canonical sampling through velocity rescaling," J. Chem. Phys. **126**, 014101 (2007). https://doi.org/10.1063/1.2408420
[50] Y.-K. Kwon, and P. Kim, *Unusually High Thermal Conductivity in Carbon Nanotubes*, in *High Thermal Conductivity Materials*, edited by S.L. Shindé, and J.S. Goela (Springer, New York, NY, 2006), pp. 227–265.
[51] A. Sharma, A. Patwardhan, K. Dasgupta, and J.B. Joshi, "Kinetic study of boron doped carbon nanotubes synthesized using chemical vapour deposition," Chem. Eng. Sci. **207**, 1341-1352 (2019). https://doi.org/10.1016/j.ces.2019.06.030
[52] M.M.S. Fakhrabadi, A. Allahverdizadeh, V. Norouzifard, and B. Dadashzadeh, "Effects of boron doping on mechanical properties and thermal conductivities of carbon nanotubes," Solid State Commun. **152**, 1973-1979 (2012). https://doi.org/10.1016/j.ssc.2012.08.003
[53] P. Ayala, *et al*., "Tailoring N-Doped Single and Double Wall Carbon Nanotubes from a Nondiluted Carbon/Nitrogen Feedstock," J. Phys. Chem. C **111**, 2879-2884 (2007). https://doi.org/10.1021/jp0658288
[54] W. Su, X. Li, L. Li, D. Yang, F. Wang, X. Wei, W. Zhou, *et al*., "Chirality-dependent electrical transport properties of carbon nanotubes obtained by experimental measurement," Nat. Commun. **14**, 1672 (2023). https://doi.org/10.1038/s41467-023-37443-7
[55] U. Khalilov, A. Bogaerts, B. Xu, T. Kato, T. Kaneko, and E. C. Neyts, "How the alignment of adsorbed ortho H pairs determines the onset of selective carbon nanotube etching," Nanoscale, **9**, 1653-1616 (2017). https://doi.org/10.1039/C6NR08005G
[56] N.R. Abdullah, H.O. Rashid, M.T. Kareem, C.-S. Tang, A. Manolescu, and V. Gudmundsson, "Effects of bonded and non-bonded B/N codoping of graphene on its stability, interaction energy, electronic structure, and power factor," Phys. Lett. A **384**, 126350 (2020). https://doi.org/10.1016/j.physleta.2020.126350
[57] X. Sha, B. Jackson, and D. Lemoine, "Quantum studies of Eley–Rideal reactions between H atoms on a graphite surface," J. Chem. Phys. **116**, 7158-7169 (2002). https://doi.org/10.1063/1.1463399
[58] T. Zecho, A. Güttler, X. Sha, D. Lemoine, B. Jackson, and J. Küppers, "Abstraction of D chemisorbed on graphite (0001) with gaseous H atoms," Chem. Phys. Lett. **366**, 188-195 (2002). https://doi.org/10.1016/S0009-2614(02)01573-7

APPENDIX
Supplementary information

Table 1. Partial charge variation with boron (B) atom doping at different temperatures for B-DWNT(5.5@10.10)

Boron doping (%)	Partial charge 300 K	Partial charge 600 K	Partial charge 900 K	Partial charge 1200 K	Partial charge 1500 K
0%	0.00	0.00	0.00	0.00	0.00
1%	~0.032	~0.041	~0.053	~0.065	~0.074
2%	~0.072	~0.088	~0.108	~0.128	~0.168
3%	~1.025	~1.102	~1.172	~1.207	~1.236
4%	~1.188	~1.212	~1.258	~1.298	~1.327
5%	~1.963	~1.984	~1.997	~1.901	~1.478
6%	~2.351	~2.382	~2.456	~2.516	~2.597
7%	~2.457	~2.484	~2.572	~2.646	~2.728
8%	~3.563	~3.602	~3.711	~3.782	~3.891
9%	~4.690	~4.727	~4.843	~4.933	~4.904
10%	~4.830	~4.867	~4.996	~5.096	~5.233

Table 2. Thermal conductivity variation with boron (B) atom doping at different temperatures for B-DWNT(5.5@10.10)

Boron Doping (%)	Thermal conductivity coefficient (W/m·K)				
	300 K	600 K	900 K	1200 K	1500 K
0%	3564	2115	1313	1140	916
1%	3512	2087	1277	1077	815
2%	3442	2052	1214	1064	783
3%	3321	1995	1165	936	593
4%	3257	1737	1012	751	464
5%	3173	1533	764	613	379
6%	2956	1395	702	478	278
7%	2818	1067	590	346	186
8%	2734	982	425	197	103
9%	2577	765	282	94	73
10%	2479	668	245	78	61

ПРОВІДНІСТЬ У ДВОСТІННИХ ВУГЛЕЦЕВИХ НАНОТРУБКАХ

Шахнозахон Мумінова[a], Аброр Улукмурадов[b], Хамід Ісаєв[b], Ділдора Мамаєва[b], Уткір Ульджаєв[a,b]

[a]Денауський інститут підприємництва та педагогіки, м. Денау, 360, Сурхандар'їнська область, 190507, Узбекистан

[b]Ташкентський інститут текстильної та легкої промисловості, Ташкент, 100100, Узбекистан

У цьому дослідженні вивчається вплив легування бором (B) на електро- та теплопровідні властивості одностінних вуглецевих нанотрубок (DWNT) за різних температур (від 300 K до 1500 K). Було проаналізовано включення атомів бору в DWNT (5,5)@(10,10), щоб дослідити, як різні рівні легування (ρ%) впливають на розподіл часткового заряду та теплопровідність. Наші результати показують, що легування бором збільшує частковий заряд у структурі нанотрубки, з нелінійним збільшенням заряду зі збільшенням концентрації легування від 0% до 10%. Це пов'язано з нижчою електронегативністю бору, який вводить носіїв дірок та посилює поведінку напівпровідника p-типу. Однак, при вищих концентраціях легування (вище 5%), дефекти порушують π-електронну мережу, зменшуючи електропровідність. Експерименти з теплопровідності показують, що присутність бору призводить до зниження ефективності теплопередачі, особливо при вищих рівнях легування (>6%), де індуковане дефектами розсіювання фононів значно знижує теплопровідність. Результати демонструють, що легування бором має складний вплив на структурні, електронні та теплові властивості DWNT, причому температура та концентрація легування відіграють вирішальну роль у визначенні характеристик.

Ключові слова: *двостінна вуглецева нанотрубка; легування бором; реактивна молекулярна динаміка*